MULTISCALE MODELING OF RADIATION EFFECTS ON MATERIALS: PRESSURE VESSEL EMBRITTLEMENT

JUNHYUN KWON*, GYEONG-GEUN LEE and CHANSUN SHIN
Korea Atomic Energy Research Institute
1045 Daedeokdaero, Yuseong-Gu, Daejeon 305-353, Korea
*Corresponding author. E-mail : jhkwon@kaeri.re.kr

Received January 15, 2009

Radiation effects on materials are inherently multiscale phenomena in view of the fact that various processes spanning a broad range of time and length scales are involved. A multiscale modeling approach to embrittlement of pressure vessel steels is presented here. The approach includes an investigation of the mechanisms of defect accumulation, microstructure evolution and the corresponding effects on mechanical properties. An understanding of these phenomena is required to predict the behavior of structural materials under irradiation. We used molecular dynamics (MD) simulations at an atomic scale to study the evolution of high-energy displacement cascade reactions. The MD simulations yield quantitative information on primary damage. Using a database of displacement cascades generated by the MD simulations, we can estimate the accumulation of defects over diffusional length and time scales by applying kinetic Monte Carlo simulations. The evolution of the local microstructure under irradiation is responsible for changes in the physical and mechanical properties of materials. Mechanical property changes in irradiated materials are modeled by dislocation dynamics simulations, which simulate a collective motion of dislocations that interact with the defects. In this paper, we present a multiscale modeling methodology that describes reactor pressure vessel embrittlement in a light water reactor environment.

KEYWORDS : Embrittlement, Multiscale Model, Molecular Dynamics, Kinetic Monte Carlo, Dislocation Dynamics

1. INTRODUCTION

Defect generation due to irradiation in nuclear power reactor materials gives rise to microstructural evolution and results in changes in material properties. When a high-energy particle collides with lattice atoms in a solid, the displacement reactions produce non-equilibrium point defects within a range of nanometer for several picoseconds. Such defects diffuse over macroscopic length and time scales and develop into a full-fledged microstructure by interacting with other extended defects. These defects significantly alter the materials chemistry and microstructure. Changes in microstructure are responsible for dimensional stabilities and mechanical property changes, including swelling, creep, and hardening. Irradiation changes the microstructure and property of materials, thereby degrading the integrity of structural components and eventually causing safety problems. In particular, the embrittlement of reactor pressure-vessel steels is a technologically and economically important issue that affects the safety and determines the lifetime of nuclear power plants.

Most problems in irradiated materials originate from the atomic collision of high-energy particles and lattice atoms. This collision leads to displacement cascades through the energy transfer reaction and causes various types of defects such as vacancies, interstitials, and clusters. The behavior of the point defects created in the displacement cascades is important in that these defects play a major role in the microstructural evolution and changes of a material property. The key to understanding and predicting mechanical property changes during irradiation is a detailed knowledge of the material's microstructures as it evolves during irradiation and the link between the microstructure and the mechanical properties [1-3]. The pertinent processes include a wide range of dimensions from atomic size to a structural component that spans more than 15 orders of magnitude. The time scale also extends over a wide magnitude, from femtoseconds (10^{-15} s) to decades. Because the reactions involved in radiation damage occur over wide scales of length and time, it is not possible to describe the damage processes through a direct experimental study.

An effort has been directed at developing improved methods for predicting embrittlement and solving related problems. Most of the previous work was empirical but, over the last few decades, the fundamental research on the underlying damage mechanisms has been a focal point. In recent years, rapid advances have been made in the computational capabilities for a realistic simulation of

complex physical phenomena. At the same time, progress has been made in understanding the effect of radiation on metals, especially iron-based alloys. Recent innovations in computational modeling, coupled with improved experimental tools, provide a basis for developing a multiscale model of pressure-vessel embrittlement. In this study, we present some of our ongoing work in this area, particularly with regard to multiscale modeling for evaluating microstructural evolution and mechanical property changes during irradiation. The next section describes a hierarchical modeling approach, starting from molecular dynamics (MD), kinetic Monte Carlo (KMC) and dislocation dynamics (DD) simulations. It is believed that this computational modeling approach can be applied to other nuclear power systems, including the currently operating light water reactors, GEN-IV nuclear power reactors, and further nuclear fusion systems.

2. MULTISCALE MODELING METHODOLOGY

The modeling methodology involves a hierarchical approach which integrates MD simulations, KMC methods, and DD simulations. Each model covers the relevant length and time scales to estimate the fate of defects and solutes, and to predict a microstructural evolution during irradiation in materials. Through the prediction of the material microstructure, it is possible to quantitatively predict radiation hardening and the post-yield deformation behavior by applying three-dimensional DD simulations. Fig. 1 provides a simplified schematic view of a multiscale modeling approach [4]. This approach is based on an information exchange, starting from the atomic to real structural length and time scales. The main objective of this approach is to track the fate of defects, impurities and solutes under irradiation and to predict the microstructural evolution. The features of microstructure can be used as a basis for modeling the mechanical behavior of materials through DD and finite element methods. The passing of information and parameters between each model is important for achieving the goal of multiscale modeling. For example, MD simulations can yield information about primary damage, particularly in terms of the cascade efficiency, the spatial distribution of point defects and the number density of defect clusters. All this information is used as input in subsequent models such as KMC and DD simulations. Because the primary damage is totally dependent on the interatomic potential used, the use of suitable parameters in multiscale simulations is important. Multiscale modeling is not sufficient to predict the performance of commercial alloys composed of various elements. Hence, an experiment is required in conjunction with the modeling. The experimental techniques that complement multiscale modeling include positron annihilation spectroscopy, small-angle neutron scattering and transmission electron microscopy for microstructural characterization, as well as tensile, creep and fracture tests for measuring the mechanical properties of irradiated materials.

2.1 MD Simulations-Primary Damage Production

The physics of primary damage production has been studied extensively by means of MD simulations and theoretical work. Displacement cascades are caused by high-energy particles such as neutron, alpha, proton or heavy ions. In light water reactor environments, fast neutrons play a role in initiating displacement cascades. In this work, the formation of primary damage to reactor

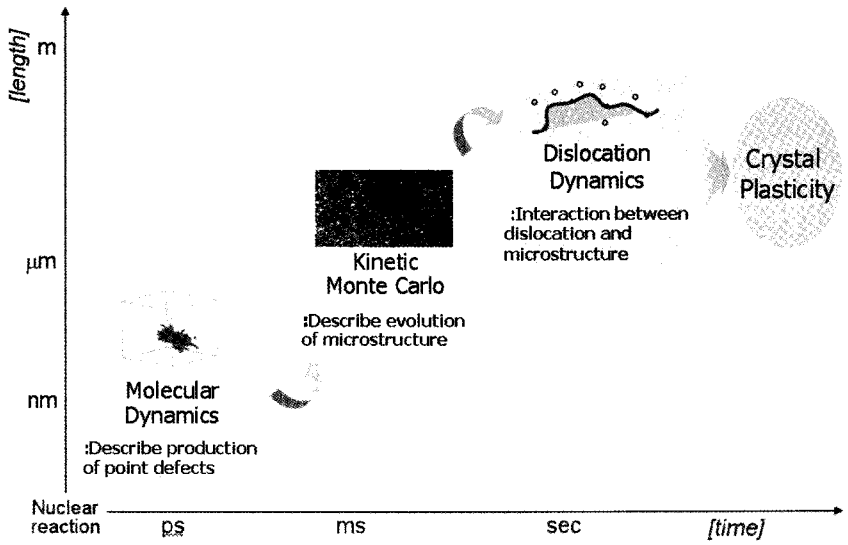

Fig. 1. Illustration of Multiscale Modeling for Radiation Damage Simulations

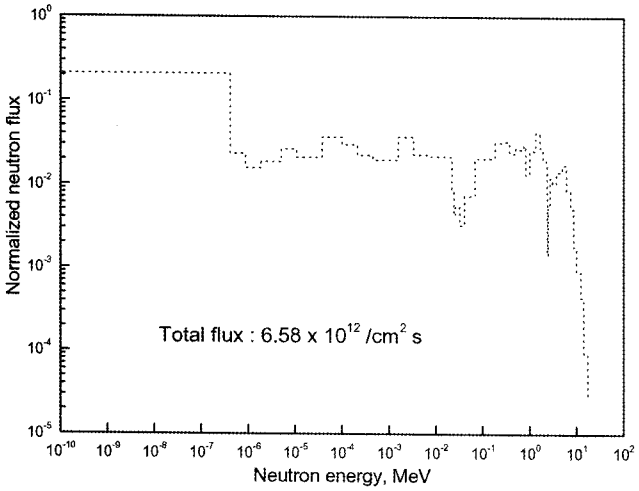

Fig. 2. Normalized Neutron Spectra for a Reactor Pressure Vessel at YG5

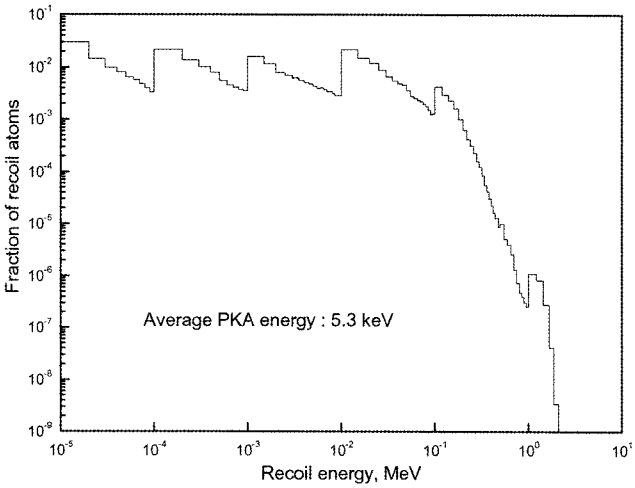

Fig. 3. Energy Spectra of PKA Atoms of Iron at YG5. The Spectral-Averaged PKA Energy is 5.3 keV

pressure vessel (RPV) steels is investigated under neutron irradiation. We use a typical set of neutron spectra for the inner surface of an RPV at Young-gwang 5 (YG5) nuclear reactor in the MD simulations. Fig. 2 shows a normalized neutron spectrum for YG5; the spectrum clearly shows the relative amount of neutron flux as a function of neutron energy. The fraction of high-energy neutrons ($E_n > 1$ MeV) that is influential in inducing the displacement cascades is about 22 percent.

Neutron damage to materials begins with the creation of primary knock-on atoms (PKAs) from high-energy neutron-nuclear interactions. The PKA spectrum is determined by such factors as the incident neutron energy, the masses involved, and the angle between the incident neutron and the recoil direction. We can readily obtain the PKA spectrum of various elements for a given neutron spectrum from the SPECTER code calculation [5]. The SPECTER code contains libraries of preprocessed cross sections for atomic displacements and gas production, as well as atomic recoil energy distributions on a specified hundred-point neutron energy grid. Accordingly, for a given neutron energy spectrum, the code simply calculates the parameters of the spectral-weighted radiation damage by converting the master library files into a user group structure. We obtained the basic parameters of radiation damage from the SPECTER code calculations by inputting the neutron spectra given in Fig. 2. The calculated displacement rate is 1.83 x 10^{-9} dpa/s and the average PKA energy for iron is 5.3 keV. Fig. 3 plots PKA recoil spectra for iron at YG5; the plot is based on calculations from the SPECTER code.

The MD method is a powerful technique for simulating displacement cascades in ordered materials. We applied the MOLDY code to simulate the displacement cascades for the primary damage evaluation [6]. In the MOLDY program, the many-body interatomic potential for BCC-Fe derived by Finnis and Sinclair is built-in [7]. This empirical potential involves two short-range interatomic terms: the sum of a repulsive term and a cohesive one. The energy per atom in a crystal is given by

$$E = \frac{1}{2}\sum_{i\neq 0} V(R_i) - A\rho^{1/2} \quad (1)$$

$$\rho = \sum_{i\neq 0} \phi(R_i), \quad (2)$$

where A is a constant, R_i is the distance between two atoms, V represents the repulsive pair potential, ϕ is the cohesive potential function, and ρ represents the cohesion which is summed over neighboring atoms, and the square-root of ρ describes the bonding energy. The Finnis-Sinclair functions are effective when R_i is greater than $0.866a_o$, where a_o is the lattice constant. For $R_i < 0.866a_o$, the universal screened Coulomb potential and the Born-Mayer potential are approximated.

The MOLDY code works with constant pressure periodic boundary conditions and uses a computational block, the size of which is determined by the given PKA energy. The link cell method is used to generate the neighboring tables for the interactions between the atoms, and only the interactions between the neighboring link cells are considered. The optimum choice for the size of each link cell is the range of the potential. Basically, the size of a link cell is slightly larger than that of a computational box so that the box can accommodate an integral number of link cells. The equations for the motions of the atoms are numerically integrated by a fourth-order

predictor-corrector algorithm for as many time steps as required. The MOLDY program has a subroutine that automatically controls the variable time step. The time step becomes large, from the smallest value of 0.01 fs, as the energy exchange between the atoms diminishes. An atomic block of the desired size is thermally equilibrated before the cascade simulations start. This process allows for the lattice vibrations of the atomic system at the simulated temperature, which takes several picoseconds. The atomic block can be used as the starting point for subsequent cascade simulations. We can initiate the cascade simulations by giving a certain amount of energy to an atom, PKA, in a specified direction. Because the choice of a different PKA or its initial direction can bring about a statistical variation, a sufficient number of simulations are required to obtain the average parameters at a given PKA energy and temperature [8].

As shown in Fig. 3, the value of 5.3 keV represents the average PKA energy for the YG5 irradiation conditions. However, this value cannot be used as the damage energy in the MOLDY code because the MOLDY code fails to account for the loss of energy caused by ionization and electronic excitation. Only a fraction of the PKA energy (E_{pka}) contributes to the cascade reaction with elastic collisions. As the input energy in the MOLDY computation, this initial kinetic energy is analogous to the damage energy (T_{dam}) in a standard Norgett-Robinson-Torrens model [9]. The relation between the PKA energy and the damage energy is given by

$$\frac{T_{dam}}{E_{pka}} = \frac{1}{1+\lambda\, w(E^+)}, \qquad (3)$$

where λ is given by $\lambda = 0.0876\, Z^{1/6}$ and Z is the atomic number. The function $w(E^+)$ is

$$w(E^+) = E^+ + 0.402(E^+)^{3/4} + 3.4(E^+)^{1/6}, \qquad (4)$$

and the variable E^+ can be written in terms of E_{pka} and Z as follows:

$$E^+ = \frac{E_{pka}}{0.0869\, Z^{7/3}}, \quad E_{pka} \text{ in keV.} \qquad (5)$$

The MD simulation energy is identical to the calculated value of the damage energy. The PKA energy of 5.3 keV corresponds to 4.09 keV of energy for the MD simulation of iron.

We performed cascade simulations until the phase of the in-cascade recombination of interstitials and vacancies was finished. After the recombination phase, however, the atomic block did not return to the thermal equilibrium state because of the high temperature. As a result, the MD simulation should be terminated when a slight change occurs in the number of point defects. For the MD simulation, the parameter of primary interest is the distribution of residual point defects after the in-cascade recombination. These residual defects are known to cause microstructural changes to irradiated material. Fig. 4 illustrates the evolution of the displacement reactions in the 5.3 keV PKA cascade; the figure shows each step from the beginning of a cascade to its relaxation in iron at 563 K. The number of point defects reaches a peak at about t = 0.30 ps. When the recombination of interstitials and vacancies starts to occur, the number of point defects decreases gradually. A constant number of stable defects could not be obtained until t = 10 ps for the 5.3 keV cascade. Of about 1200 displaced atoms at the peak of the cascade, about 40 interstitials remained at the end, which is a phenomenon similar to that of the vacancies.

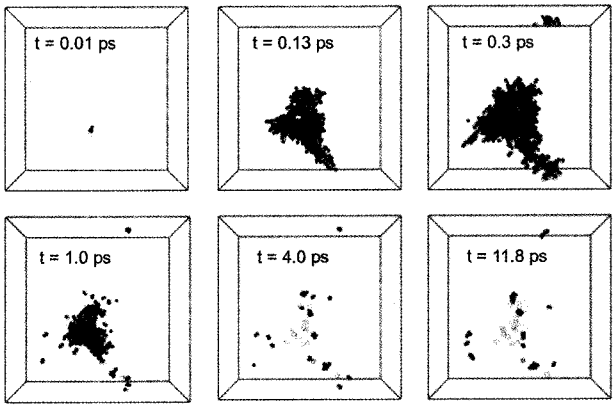

Fig. 4. Evolution of Displacement Cascade from a 5.3 keV MD Simulation in α-Iron at 563 K as a Function of Time. The Block Size is $40a_o$ x $40a_o$ x $40a_o$ (a_o: Lattice Constant) and the Initial PKA Direction is [135]. The Filled Dots Represent Interstitials; the Empty Dots Represent Vacancies.

For the given value of the PKA energy, we performed six simulations with different positions and different initial PKA directions. For two different initial PKA positions, we considered three directions: [135], [123], and [111]. The size distribution of the point defect clusters, which was derived by averaging the six simulation results, fails to show a strong dependency on the initial direction and the PKA position. Fig. 5(a) shows the vacancy cluster distribution in α-Fe. Seventy percent of the residual vacancies tend to form single point defects in the primary damage state. On the other hand, as shown in Fig. 5(b), a higher portion of interstitials form clusters, albeit small ones. The clustering formation of the interstitials is significant because these defects are thermally stable and can migrate away from the region of their parent cascade to be absorbed preferentially at such sinks as dislocations and grain boundaries. In contrast, vacancy clusters are

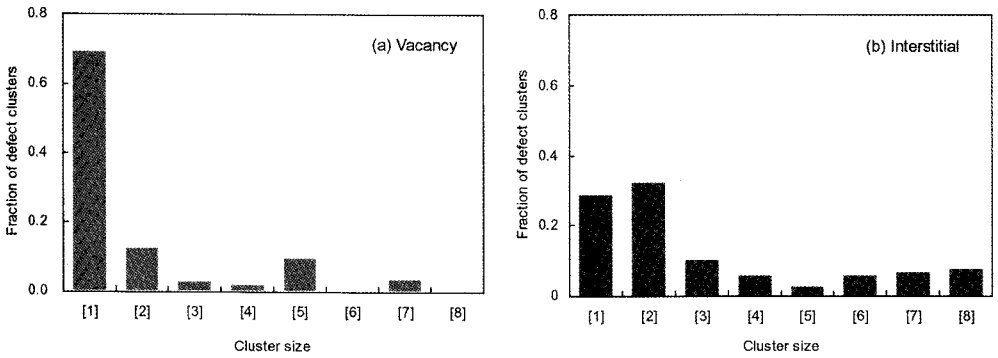

Fig. 5. Distribution of Residual Point Defects as a Result of Displacement Cascades: (a) Vacancy and (b) Interstitial. The Data Plotted above is Averaged over Six MD Simulations in BCC-Iron at a PKA Energy of 5.3 keV.

unstable and tend to be dissociated into single point defects at high temperature. Several parameters were derived from the results of the MD computation. We obtained the cascade efficiency by dividing the number of Frenkel pairs produced in the primary damage state by the number obtained from the Norgett-Robinson-Torrens formula. Generally, the cascade efficiency, which accounts for the in-cascade recombination, decreases as the PKA energy increases. In the MD simulation, we found that a certain fraction of point defects exists as clusters. For interstitial clusters, we evaluated the in-cascade clustering fractions according to the size of the interstitials and determined the vacancy-clustering fraction as a single value by assuming that all vacancy clusters were created with the same size. Table 1 lists the important parameters from the MD computation that are used in the subsequent model calculation, as in the KMC and DD simulations.

2.2 KMC Simulations-Microstructural Evolution

The major problems in materials science are closely related to changes in structure and properties over time. In general cases, an MD simulation can accurately describe the atomistic behavior but the total simulation time is typically limited to less than 1 ms. On the other hand, the processes we wish to study and observe often occur in much longer time scales. These processes include reactions between atoms, adsorption-desorption on the surface, occasional transitions from one state to another, and especially diffusion and annihilation of defects after a cascade event in an irradiation experiment. These events take much longer than general events such as an atomistic thermal vibration. This problem is called a time-scale problem and these types of processes are called rare events. KMC simulations attempt to overcome this limitation by exploiting the fact that the long-term dynamics of this kind of system typically consist of jumps from state to state [10]. A KMC simulation can reach vastly longer time scales, typically in the region of seconds and often much longer. The KMC calculation needs parameters about the rates of events: diffusion, formation of defects, dissociation of particles, and so on. However, the KMC method itself cannot predict the rates of these parameters. This information can be acquired by an ab initio calculation or MD simulation. Fig. 6 shows the various events considered in the KMC method [11].

Table 1. Data for Primary Damage as a Result of 5.3 keV Displacement Cascades for α-Iron at 563K

Cascade efficiency	0.64
Vacancy clustering fraction	0.31
Number of vacancies per initial vacancy cluster	3
Di-interstitial clustering fraction	0.32
Tri-interstitial clustering fraction	0.1
Tetra-interstitial clustering fraction	0.06

The time progress in the KMC simulation is known by different sources such as the residence-time algorithm or the Bortz-Kalos-Liebowitz algorithm [10]. In the KMC simulation, we can directly compare the stochastic simulation results with the experimental results. Fig. 7 shows the basic KMC algorithm. Firstly, the frequencies of all events are converted as rates. A list of all possible rates in the system is decided before running the simulation. The total event rates are accumulated to estimate the elapsed time. An event to be conducted is chosen by using a uniform random number. The elapsed time is updated in inverse proportion to the total event rates. After the chosen event is carried out, the list of events and total event rates are updated and the simulation is repeated until the target dose or time is reached.

As an application of the KMC algorithm on the microstructural evolution, the effect of temperature on the microstructural evolution in the ferrite phase was analyzed in this study. The ferrite phase was assumed to be pure Fe, and the model parameters based on the works

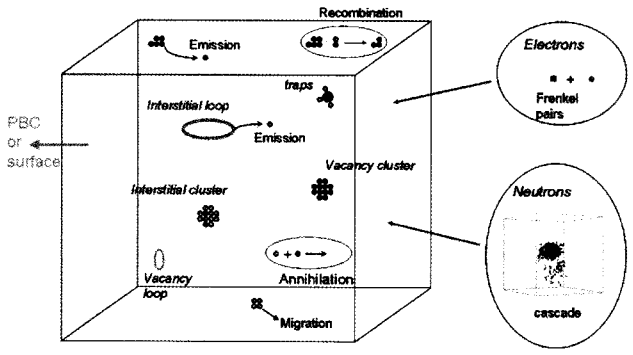

Fig. 6. The Various Events in a KMC Simulation

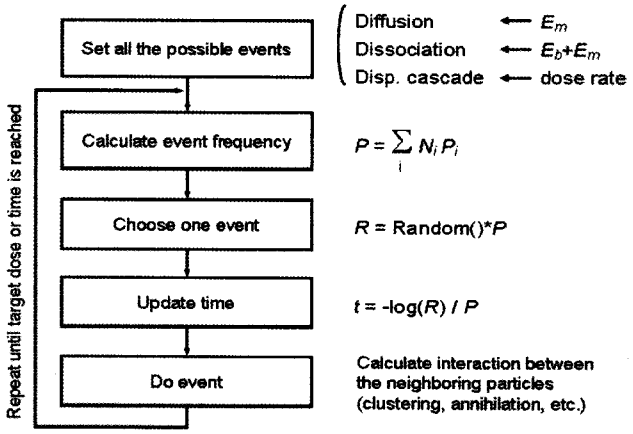

Fig. 7. Schematic of the KMC Algorithm

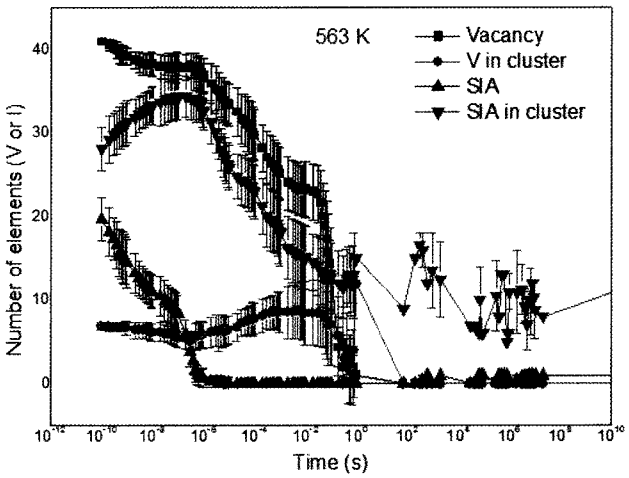

Fig. 8. The Number of Elements with Time during the Annealing of a 20 keV Cascade in Fe

of Soneda [12] and Caturla [13] were used in the simulation. Firstly, we investigated the annealing of one cascade with an energy level of 20 keV. Fig. 8 shows the distribution of the defects during the annealing. The time scale is spread over about 10^{20} s, and the error bars correspond to the standard deviation. Because of the characteristics of Monte Carlo methods, we conducted 10 cascade ageing simulations with the same initial configuration but with different random number seeds. The graph is divided into four regions. Region 1 (10^{-10} s to 10^{-6} s) is related to the migration of self-interstitial atom (SIA). Because its jump activation energy is very low, an SIA can move easily and quickly during a simulation. The mobile SIA reacts with other defect, resulting in the formation of an SIA cluster or the elimination by the reaction with vacancy species. The number of SIA clusters increases and the number of vacancies and V clusters decrease with time. However, most of the SIAs are removed at the boundaries because the simulation box is limited with dimensions of 200 nm × 200 nm × 200 nm by 10^{-6} s. Region 2 (10^{-6} s to 10^{-1} s) is connected to the diffusion of single vacancies. Because the jump activation energy has a rather high value (0.87 eV), the diffusion of vacancies starts at 10^{-6} s and ends at 10^{-1} s. Many single vacancies are removed at the boundary of the simulation box, and other vacancies react with clusters of defects. The size of the vacancy clusters increases over time, and the immobile SIA clusters decrease with the reaction of single vacancies. All the mobile species are removed from the simulation box by this time. Region 3 (10^{-1} s to 10^{1} s) indicates the dissociation of V clusters. Immobile V clusters are thought to be unstable at high temperature [8]. Hence, the V clusters emit a vacancy from themselves. The emitted single vacancies diffuse and react with other clusters. However, the volume fraction of the clusters is rather small, and most mobile single vacancies are removed at the boundaries. All the V clusters are dissociated at this stage. In region 4 (10^{1} s to 10^{10} s), only the SIA clusters remain because, as shown in the MD calculations, the SIA clusters have a high binding energy. These remaining SIA clusters are supposed to cause matrix damage in RPV steel [14].

The annealing behavior over time is closely related to the diffusion rate and dissociation rates. These rates are calculated on the basis of the thermal activation energies. Thus, the temperature of the system affects the distribution of defects. Fig. 9 represents the annealing behavior of a cascade at various annealing temperatures. As the temperature increases from 298 K to 600 K, the area of regions 1, 2, and 3 decreases. The diffusion of a single vacancy (Region 2) and the dissociation of the V clusters (Region 3) are considerably affected because of high activation energies. At a low temperature, a single vacancy shows a very low diffusivity and a vacancy cannot move easily. The remaining time of the single vacancies in the simulation box is extended to 10^{6} s at 298 K. The V clusters still remain at the end of simulations. As the system temperature increases, the areas of regions 2, 3 decrease drastically because of the increased diffusivity of a single vacancy. The diffusion of vacancy enhances the movement

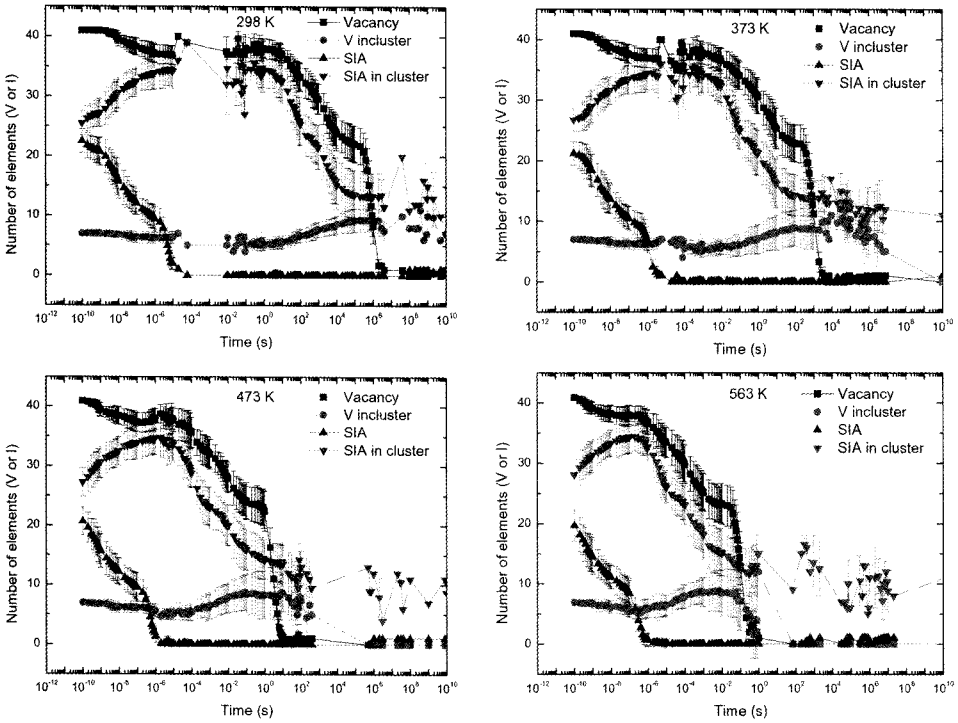

Fig. 9. The Number of Elements Versus Time with Different Annealing Temperatures

of a substitution solute atom and causes the precipitation of Cu in RPV steel. This type of precipitation is thought to be a critical factor of irradiation embrittlement. The decrease of region 1, which is related to the diffusion of single SIAs, is not really affected because of the low jump activation energy. The behavior of the SIA clusters remains unchanged with the irradiation temperature because of their high thermal stability. The high thermal stability of the SIA clusters is presumed to cause the introduction of matrix damage in the RPV steel.

When the accumulation behavior of neutron irradiation in materials is simulated, cascades should be introduced periodically in the simulation box. We introduced cascades with an energy level of 20 keV at a dose rate of 0.001 dpa/s, and the total simulation time was 1 s. The effect of the irradiation temperature on an accumulation was also analyzed. Fig. 10 shows the number densities of the defect clusters during irradiation. At a low temperature of 298

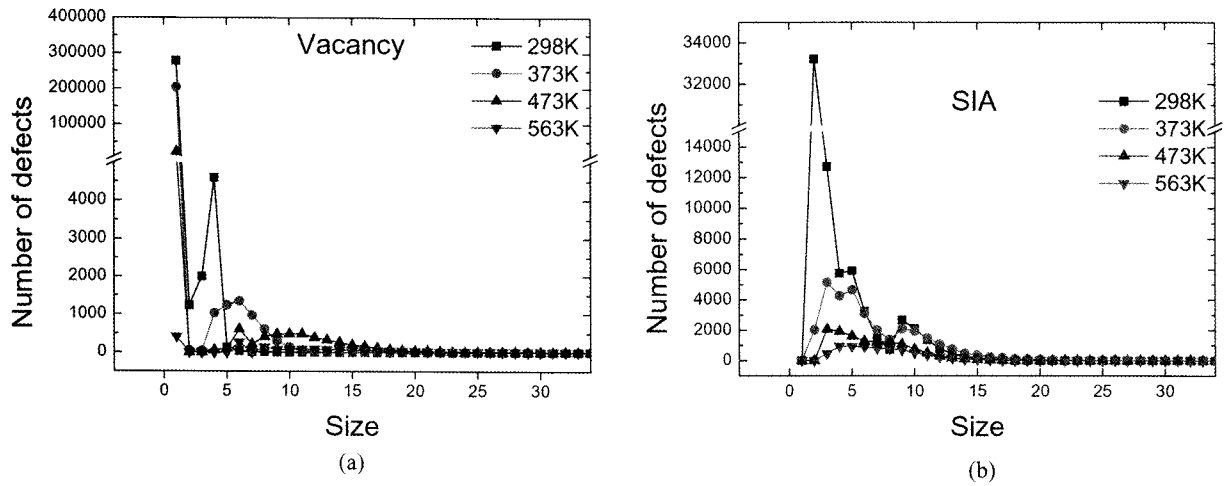

(a) (b)

Fig. 10. The Size Distribution of Defects and Defect Clusters with Various Temperatures. This Result is Calculated at the Time of 1 s: (a) Vacancy Cluster Distribution and (b) SIA Cluster Distribution.

K, there were many single vacancies in the simulation box but we could find no single SIAs because of the diffusivity differences between a vacancy and an SIA. A vacancy with a low diffusivity freezes after a cascade and is accumulated in the simulation box. The SIAs, which have small dependencies on the temperature, diffuse freely and are removed at the boundaries. As the temperature increases, the vacancies diffuse, react with sessile clusters, and disappear at the boundaries. The total number of V clusters decreases seriously at 563 K, and the mode value of the V cluster size shifts to a higher value. The number density of the SIA clusters also decreases. However, this decrease is not due to the dissociation of the SIA clusters but due to the reaction between a mobile vacancy and an immobile SIA cluster. Note also that at a temperature of 563 K the number density of the SIA clusters is higher than that of a V cluster. These remaining SIA clusters are thought to be the cause of the matrix damage on the Fe ferrite. The results confirm the usefulness of the KMC simulation for estimating microstructural evolution.

2.3 DD Simulations-Interaction between Dislocations and Microstructure

Deformation of metals can be, in theory, described as a collective motion of dislocations. A dislocation is a line defect within a crystal, which represents permanent deviations of atoms from their original crystallographic periodicity [15]. A dislocation glide induces permanent deformation; hence, a dislocation is a microscopic carrier of metallic plasticity.

The purpose of this section is to describe a general scheme for predicting radiation hardening by simulating the behavior of dislocations under irradiation and to present some of our previously published numerical studies of radiation hardening [16, 17].

DD solves the equation of motion of dislocation lines. Dislocation lines are represented by a connected set of discrete segments. In the DD code used in this work, a curved dislocation line is represented by a succession of two orthogonal dislocation segment sets [18]. Each segment generates a stress field. The stress field of a dislocation segment is obtained by using the stress field solution of a semi-infinite dislocation, a solution originally formulated in [19] and modified by Devincre [20] in compact forms. This internal stress field of each segment influences the behavior of other segments over a long range as well as the applied stress fields and lattice resistance (the Peierls stress). The segments interact with each other upon collision. These short-range interactions entail reactions such as a junction formation and the annihilation of dislocation segments. The collective evolution of a large number of interacting dislocations is simulated under an external loading in DD simulations. An individual dislocation glide causes a plastic strain in the simulation volume; hence, the stress-strain behavior is an output of the DD simulations.

The dynamics of a dislocation line are material-specific. In the case of RPV steels, which have a BCC structure, the core structure of dislocations is extended in three adjacent {110} planes [21]. This extended core structure is the origin of a high Peierls stress. A screw dislocation line moves from one Peierls valley to another by nucleation and subsequent migration of kinks along the screw dislocation line due to a high Peierls stress. This behavior is called the kink-pair mechanism [22]. The formation of kinks is a thermally activated process; hence, the velocity of a screw dislocation is temperature-dependent. The velocity of edge segments is much higher than the velocity of screw segments and is typically set to about 100 times faster than screw segments. The velocity of screw segments is expressed as follows in DD simulations in order to capture the thermally activated process involved in a motion:

$$v = A\exp\left(\frac{-\Delta H(\tau)}{k_B T}\right),\ \Delta H(\tau) = \Delta H_c\left[1-\left(\frac{\tau}{\tau_0}\right)^p\right]^q. \quad (6)$$

With the parameters ΔH_c=0.84 eV, τ_0=418.8 MPa, p=0.456, and q=1.268 for Eq. (6), we can compute the critical resolved shear stresses for pure iron. As shown in Fig. 11, the calculated data agree well with experimental data. The critical stress increases as the temperature decreases because of the decreased thermal vibration energy of atoms. A computed dislocation microstructure at T = 200 K is presented in Fig. 12. Screw dislocations are dominant at a low temperature, and the dislocation structures shown on one of the {110} slip planes (Fig. 12(b)) represent well the typical microstructure of BCC metals observed with a transmission electron microscope [23]. The effects of solutes in RPV steels can be incorporated

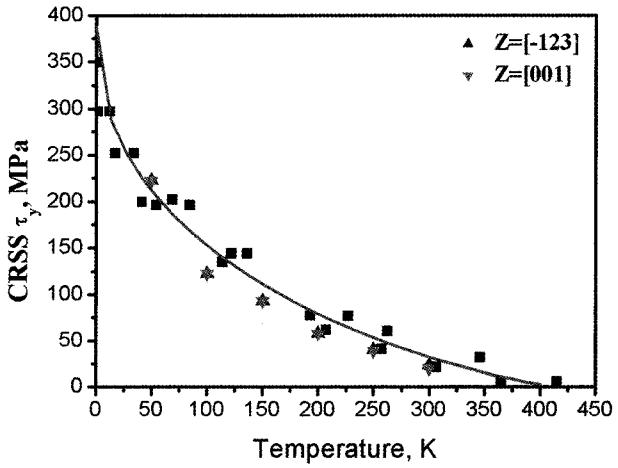

Fig. 11. Temperature Dependence of Critical Resolved Shear Stress of a Pure Iron (Square Symbols) and Simulated Tensile Test along [001] and [-123] Axis with a Strain Rate of 10^{-4}/s

by modifying the parameters (ΔH_c, τ_0, p, q), and the solution hardening or solution softening [24] due to specific solutes can be incorporated [25].

Radiation defects interact with moving dislocations and hinder the motion of dislocations. The interactions between dislocations and radiation defects are the origin of the changes in mechanical properties as well as the change in microstructure after deformation of nuclear materials, such as the formation of cleared channels.

When radiation hardening is simulated in DD simulations, two types of information need to be passed from other simulations: firstly, the density and the size distribution of radiation-induced defects and, secondly, the defect strength, i.e. the barrier strength to the dislocation motion.

Detailed information on the interactions between radiation defects and moving dislocations can be obtained by using atomistic simulations [26]. For example, as shown in Fig. 13(a), our investigation of the interactions of the Frank loop with the glide dislocation show that the loop hinders the motion of gliding dislocations [16]. The interaction of the loop and a moving dislocation can be represented in DD simulations, as shown in Fig. 13(b), by representing the loop as a plane with a predefined barrier strength to a dislocation motion.

In [17], we computed the changes of the yield strength in irradiated austenitic stainless steels by using multiscale modeling. The density and the size distribution of radiation-induced defects were computed by using the cluster dynamics model. This information was passed to the DD simulations so that the radiation defects could be distributed randomly in the simulation volume; furthermore, no clustering of the defects was considered. The defect strength, which was assumed to be size-dependent, was taken as a fitting parameter. The computed yield strengths were in good agreement with the experimental data. To build a purely predictive model of estimating radiation-induced hardening, however, we need more detailed information of defect strength, such as the effects of the clustering of defects on the motion of dislocations.

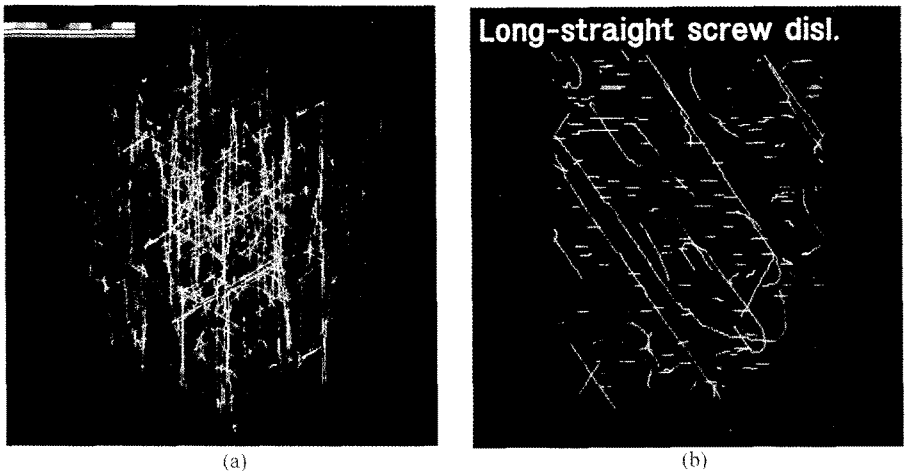

(a) (b)

Fig. 12. Dislocation Structure after the Application of Tensile Stress along [001] at 200 K in (a) a Simulation Volume in 3-D and (b) a Sliced Volume Normal to (110)

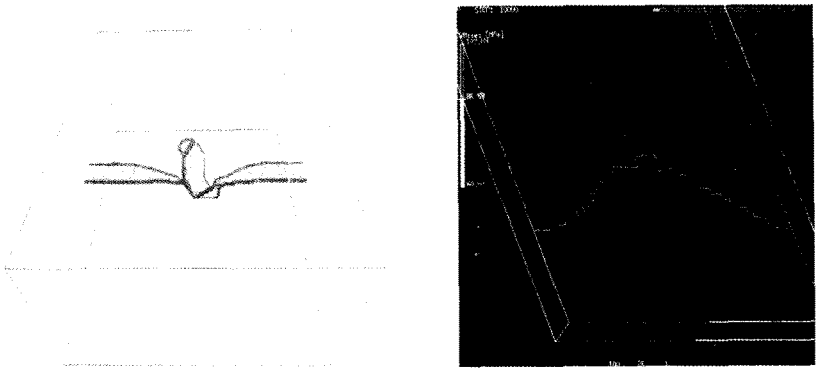

(a) (b)

Fig. 13. Simulation of the Interaction between a Frank Loop and a Glide Dislocation by using (a) MD and (b) DD

3. CONCLUSION

We have presented a multiscale modeling approach to modeling radiation damage in RPV steels. The approach is based on atomistic MD simulations, which produce the primary damage in displacement cascades, and KMC simulations, which estimate the microstructural evolution under irradiation. By using three-dimensional DD calculations, we can then find the link between the microstructure and the mechanical properties. In multiscale modeling, the passing of information between each method is critical; in particular, information on the parameters and controlling mechanisms needs to be passed from an atomic scale to micro, meso, continuum and structural scales. This paper outlines selected results from a study of multiscale modeling of RPV embrittlement. The hierarchical approach, with the integration of three models, can improve the capability of materials property changes without resorting much to irradiation tests. However, a performance test of irradiated materials is indispensible for improving multiscale modeling. Future work will focus on both areas for code validation and verification.

ACKNOWLEDGEMENTS

The authors gratefully acknowledge Dr. R.E. Stoller of the Oak Ridge National Laboratory and Dr. B.D. Wirth of University of California at Berkeley for providing the MOLDY and BIGMAC code, respectively. This research is sponsored by the Korean Ministry of Science and Technology under the National Mid-term and Long-term Atomic Energy R&D Program.

REFERENCES

[1] G.R. Odette, B.D. Wirth, D.J. Bacon, and N.M. Ghoniem, "Multiscale-multiphysics modeling of radiation-damaged materials: Embrittlement of pressure-vessel steels," *MRS Bulletin/March*, 176 (2001).

[2] B.D. Wirth, M.J. Caturla, T. Diaz de la Rubia, T. Khraishi, and H. Zbib, "Mechanical property degradation in irradiated materials: A multiscale modeling approach," *Nucl. Instr. and Meth. B*, **180**, 23 (2001).

[3] B.D. Wirth, G.R Odette, J. Marian, L. Ventelon, J.A. Young-Vandersall, and L.A. Zepeda-Ruiz, "Multiscale modeling of radiation damage in the fusion environment," *J. Nucl. Mater.*, **329-333**, 106 (2004).

[4] J .Kwon, G..-G.. Lee, and C. Shin, "Multiscale modeling approach to radiation effects on materials," *KNS and AESJ Joint Summer School 2007*, Seoul, Korea, Aug.27-30, 2007.

[5] L.R. Greenwood and R.K. Smither, "SPECTER: Neutron Damage Calculations for Materials Irradiations," ANL/FPP/TM-197, Argonne National Laboratory (1985).

[6] M.W. Finnis, "MOLDY6-A molecular dynamics program for simulation of pure metal," Harwell Report AERE R-13182 (1988).

[7] M.W. Finnis and J.E. Sinclair, "A simple empirical N-body potential for transition metals," *Phil. Mag. A*, **50**, 45 (1984).

[8] R.E. Stoller and L.R. Greenwood, "Subcascade formation in displacement cascade simulations: Implication for fusion reactor materials," *J. Nucl. Mater.*, **271&272**, 57 (1999).

[9] M.J. Norgett, M.T. Robinson and I.M. Torrens, "A proposed method of calculating displacement dose rates," *Nucl. Eng. Design*, **33**, 50 (1975).

[10] A.F. Voter, "Introduction to the kinetic Monte Carlo method," in: K.E. Sickafus and E.A. Kotomin, *Radiation Effects in Solids*, p. 1, Springer, Dordrecht (2005).

[11] C. Domain, C.S. Becquart, and L. Malerba, "Simulation of radiation damage in Fe Alloys: an object kinetic Monte Carlo approach," *J. Nucl. Mater.*, **335**, 121 (2004).

[12] N. Soneda and T. Diaz De La Rubia, "Defect production, annealing kinetics and damage evolution in α-Fe: an atomic-scale computer simulation," *Phil. Mag. A*, **78**, 995 (1998).

[13] M.J. Caturla, N. Soneda, E. Alonso, B.D. Wirth, T. Diaz de la Rubia, and J.M. Perlado, "Comparative study of radiation damage accumulation in Cu and Fe," *J. Nucl. Mater.*, **276**, 13 (2000).

[14] N. Soneda, S. Ishino, A. Takahashi, and K. Dohi, "Modeling the microstructural evolution in bcc-Fe during irradiation using kinetic Monte Carlo computer simulation," *J. Nucl. Mater.*, **323**, 169 (2003).

[15] J.P. Hirth and J. Lothe, Theory of Dislocations, Krieger Publishing Company, Malabar, Florida, 1992

[16] C. Shin, H.-H. Jin, J. Kwon, J.-H. Shim and T.S. Byun, "Mechanism for unfaulting of an extrinsic Frank loop with <112> edges by glide dislocations," *J. Kor. Phys. Soc.*, **52**, 1250 (2008).

[17] C. Shin, J. Kwon and W.W. Kim, "Prediction of radiation-induced yield stress increment in austenitic stainless steels by using a computational approach," *J. Nucl. Mater.*, in press, http://dx.doi.org/10.1016/j.jnucmat.2008.12.189.

[18] C. Shin, M.C. Fivel, M. Verdier, S.C. Kwon, "Numerical methods to improve the computing efficiency of discrete dislocation dynamics simulations," *J. Comp. Phys.*, **215**, 417 (2006).

[19] R. de Wit, "Some relations for straight dislocations," *Phys. Stat. Sol.*, **20**, 567 (1967).

[20] B. Devincre, "Three dimensional stress field expressions for straight dislocation segments", *Solid State Commun.*, **93**, 875 (1995).

[21] C. Domain and G. Monnet, "Simulation of screw dislocation motion in iron by molecular dynamics simulations," *Phys. Rev. Lett.*, **95**, 215506 (2005)

[22] J. Marian, W. Cai and V.V. Bulatov, "Dynamic transitions from smooth to rough to twinning in dislocation motion," *Nature Mater.*, **3**, 158 (2004).

[23] F. Louchet and L.P. Kubin, "Dislocation substructures in the anomalous slip plane of single crystal niobium strained at 50 K," *Acta Metall.*, **23**, 17 (1975).

[24] D. R. Trinkle and C. Woodward, "The chemistry of deformation: How solutes soften pure metals," *Science* **310**, 1665 (2005).

[25] C. Shin, H.H. Jin, *unpublished work.*

[26] Y.N. Osetsky, D. Rodney and D.J. Bacon, "Atomic-scale study of dislocation-stacking fault tetrahedron interactions. Part I: Mechanisms," *Phil. Mag.*, **86**, 2295 (2006).